

# Weakly nonlinear saturation of short-wave instabilities in a strained Lamb–Oseen vortex

Denis Sipp<sup>a)</sup>

ONERA, 29 avenue de la Division Leclerc, BP 72, F-92322 Châtillon Cedex, France

(Received 18 November 1999; accepted 5 April 2000)

A Lamb–Oseen vortex in a planar straining field is known to be subject to 3D (three-dimensional) short-wave instabilities which are due to the resonance of the straining field and two stationary Kelvin waves characterized by the same axial wave number and by azimuthal wave numbers equal to  $-1$  and  $+1$ . The linear regime has been described by Moore and Saffman (1975). In this article, we extend this analysis to the weakly nonlinear regime. The emerging eigenmode is characterized by a complex amplitude  $A = |A|e^{i\phi}$ , whose behavior is governed by an amplitude equation. It is shown that the unstable perturbation corresponds to an oscillation of the vortex in a plane inclined at an angle  $\phi$ , while the amplitude of these oscillations is proportional to  $|A|$ . The vortex centers are defined as the points where the velocity of the vortex is zero, which also corresponds to the points where the pressure is minimum. We show that these instabilities saturate. The saturation amplitudes are evaluated numerically and expressed in terms of oscillation amplitudes of the vortex centers. If  $a$  denotes the internal radius of the vortex and if the straining field is due to a counter-rotating vortex of same strength, located at a distance  $b$ , then the maximum amplitude  $\Delta$  of the vortex oscillations is  $\Delta/b = 6.1a^2/b^2$ . This result is in agreement with those of the experiments of Leweke and Williamson (1998) for which  $a/b = 0.2$ . It also shows that in aeronautical situations, for which  $a/b$  is smaller, i.e.,  $a/b < 0.1$ , the considered short-wave instability will saturate at very low amplitude.

© 2000 American Institute of Physics. [S1070-6631(00)02607-6]

## I. INTRODUCTION

The experiments of Leweke and Williamson<sup>1</sup> show two counter-rotating vortices subject to two kind of instabilities. First, the long wave instability, also called the Crow instability, is characterized by symmetric oscillations with an axial wavelength comprised between  $5b$  and  $10b$ , where  $b$  is the distance between the two vortices. The linear regime has been described by means of filament vortex methods by Crow, Moore, Saffman, and Widnall.<sup>2–7</sup> Secondly, the short-wave instability, for which the axial wavelength is approximately equal to the internal radius  $a$  of the vortices, has been analyzed by Moore and Saffman.<sup>8</sup> These authors considered an axisymmetric vortex in a weak planar straining field, which models the presence of the other vortex. It is shown that linear instability may arise through the resonance of the straining field with two stationary Kelvin waves of the same axial wave number and with azimuthal wave numbers  $-1$  and  $+1$ . The case of the Rankine vortex was considered in details by Tsai and Widnall<sup>9</sup> while the Lamb–Oseen vortex was treated by Eloy and Le Dizès.<sup>10</sup> In both studies, numerical values of the amplification rates and of the unstable axial wave numbers have been given. These instabilities belong to a more general family, called the elliptic instabilities. Pierrehumbert,<sup>11</sup> Bayly,<sup>12</sup> and Waleffe<sup>13</sup> showed that a planar flow with constant vorticity and elliptic streamlines was subject to broadband instabilities. They have exhibited an unstable eigenmode concentrated in the neighborhood of the

elliptic stagnation point, with the horizontal vorticity of the eigenmode lying in the stretching direction of the basic flow and the vertical vorticity forming a dipole structure. Such an eigenmode has been identified in the experiment of Leweke and Williamson.<sup>1</sup>

The nonlinearities modify the dynamics of the emerging unstable eigenmode. Different behaviors may be expected, e.g., a saturation of the linearly unstable eigenmode. Observations, experiments and simulations<sup>14</sup> show that the Crow instability does not saturate and that its development leads to the formation of vortex rings. This behavior has been explained by Klein *et al.*<sup>15,16</sup> Similarly, the experiments of Leweke and Williamson<sup>1</sup> as well as the direct numerical simulations of Orlandi *et al.*<sup>17</sup> suggest that the short-wave instabilities do not saturate. One observes in both cases that the vortices are subject to large amplitude oscillations. We are going to prove in this article, that these instabilities actually saturate, but that the corresponding saturation amplitudes are very large when the dipole aspect ratio  $a/b$  is not small enough, as in the two references mentioned above. We will prove that if one considers lower values of  $a/b$ , typically  $a/b < 0.1$ , then the saturation amplitudes will be much smaller.

In the case of a rotating elastic cylinder subject to an elliptical distortion, Malkus<sup>18</sup> observed that unstable waves are seen to grow for some time and then dramatically collapse into small-scale disorder. In order to explain such a behavior, Waleffe<sup>19</sup> achieved a weakly nonlinear analysis of the elliptic instability developing in a flow in body rotation subject to a weak elliptical distortion. He showed that the

<sup>a)</sup>Electronic mail: sipp@onera.fr

elliptic instability should saturate, which is apparently in contradiction with the experiment. This paradox has been recently explained by Kerswell<sup>20</sup> and Mason and Kerswell.<sup>21</sup> They show by means of direct numerical simulations that one cannot actually observe the weakly nonlinear saturated states because they are either unstable to secondary instabilities at observable amplitudes or neighboring competitor elliptical instabilities grow to ultimately disrupt them. Similar mechanisms are expected in the case of short-wave instabilities developing in vortex pairs, but they have not yet been observed. The maximum development of the short-wave instabilities is thought to be limited either by the nonlinear saturation or by the early development of secondary instabilities. The present paper is devoted to the evaluation of the amplitude of the saturated states and its dependence with respect to the dipole aspect ratio  $a/b$ .

Several studies concerning the weakly nonlinear regime of the elliptic instability already exist. The first one is due to Waleffe<sup>19</sup> who treated the case of a bounded strained but uniform vortex. The constructed amplitude equations in the latter work show that the elliptic instability saturates due to a nonlinear phase shifting from the direction of stretching. In the present paper, which deals with a nonbounded strained vortex with a radial structure, we find similar amplitude equations but with different numerical constants. Therefore, the qualitative features of the weakly nonlinear development of the elliptic instability that are described in this paper are the same as those presented by Waleffe. The two physical problems—case of a bounded strained but uniform vortex and case of a nonbounded strained vortex with radial structure—are actually very similar. Instability occurs in both situations because of deformations that reduce the symmetry of the system. In the context of Hamiltonian systems, Guckenheimer and Mahalov<sup>22</sup> and Knobloch *et al.*<sup>23</sup> thoroughly analyzed this generic situation. On grounds of symmetry, these authors have found amplitude equations whose structure is the same as that found by Waleffe and that found in the present paper. Since the equations of fluid dynamics play no explicit role in the derivation of their results, it is interesting in the present paper to discuss their approach with respect to a true fluid-dynamical situation. Finally, Lebovitz and Saldanha<sup>24</sup> stressed the fact that all the works mentioned above only describe local bifurcations. They showed that the weakly non-linear development of elliptic instability could also lead to global bifurcations of the system, depending on the linear instabilities that are considered.

Note that the flow will be considered as inviscid so that the incompressible Euler equations will be used. Viscosity does not play an important role in the basic physics of the elliptic instability. The inviscid analysis presented in this paper actually holds even if the flow is weakly dissipative—one has to consider sufficiently high Reynolds numbers. This stems from the fact that no boundaries are considered here and that all velocity profiles are infinitely smooth.

The paper is organized as follows. In Sec. II, we present the weakly nonlinear analysis, which is based on a multiple time scale analysis. We consider an expansion for the velocity field, which includes two small parameters, the intensity of the straining field  $\epsilon$  and the amplitude  $\alpha$  of the 3D pertur-

bations. We recall briefly how the vortex adapts<sup>8</sup> to the presence of the straining field and present the essential ideas used afterwards to construct the amplitude equations. In Sec. III, we give these amplitude equations as well as the numerical values of the involved constants. We only present the results, the details of the weakly nonlinear analysis being postponed to Appendix A. In Sec. IV, we analyze the qualitative dynamics of the system in the phase space, which is three-dimensional here. In particular, the well-known features of the linear short-wave instability will be retrieved and the saturation process presented by Waleffe<sup>19</sup> will be recalled. The results will also be discussed in the light of those obtained by Guckenheimer and Mahalov.<sup>22</sup> Section V is devoted to the application of these results to the case of a vortex pair. In particular, it will be shown that for small aspect ratios  $a/b$ , as obtained in real aircraft wake vortices, the considered short-wave instability saturates at very low amplitude.

## II. PRESENTATION OF THE WEAKLY NONLINEAR ANALYSIS

We consider an asymptotic expansion of the velocity field  $\mathbf{u}$  with two small parameters  $\epsilon$  and  $\alpha$  of the form

$$\mathbf{u} = \underbrace{\mathbf{u}_0 + \epsilon \mathbf{u}_1 + \dots}_{\text{Steady 2D strained vortex}} + \underbrace{\alpha \mathbf{u}_{01} + \alpha^2 \mathbf{u}_{02} + \alpha^3 \mathbf{u}_{03} + \epsilon \alpha \mathbf{u}_{11} + \alpha^4 \mathbf{u}_{04} + \epsilon \alpha^2 \mathbf{u}_{12} + \dots}_{\text{Unsteady 3D perturbation}}, \quad (1)$$

$\epsilon$  designates the strength of the straining field while  $\alpha$  is the amplitude of the leading-order term of the 3D perturbation.  $\epsilon$  is an external control parameter while  $\alpha$  has to be determined in the course of the analysis as a function of  $\epsilon$ . This expansion as well as the analogous one for the pressure field are introduced in the incompressible Euler equations. For small  $\alpha$  and  $\epsilon$ , we obtain a series of equations at various orders in  $\epsilon^i \alpha^j$ . Generally speaking,  $\mathbf{u}_{ij}$  will be determined at order  $\epsilon^i \alpha^j$  by an inhomogeneous linear equation. The homogeneous part of this equation is always the same and describes the linear dynamics of the Lamb–Oseen vortex while the forcing term involves terms of lower orders, which have been determined previously. Solving the inhomogeneous equations shows that compatibility conditions for the forcing terms have to be fulfilled when the homogeneous operator is degenerate. These conditions determine the amplitude equations. Here two characteristic slow time scales will be introduced which are linked to the two basic physical mechanisms that exist here, i.e., instability developing on the characteristic time scale  $1/\epsilon$  and phase dynamics for the Kelvin waves on the time scale  $1/\alpha^2$ . The comparison between these two time scales determines the order of magnitude  $\alpha$  of the 3D perturbation:  $\alpha = \sqrt{\epsilon}$ .

The expansion (1) is compound of two parts:

- (1) The first one,  $\mathbf{u}_0 + \epsilon \mathbf{u}_1 + \dots$  is a 2D flow representing a Lamb–Oseen vortex in a straining field of strength  $\epsilon$ . In a cylindrical basis  $(\mathbf{e}_r, \mathbf{e}_\theta, \mathbf{e}_z)$ :

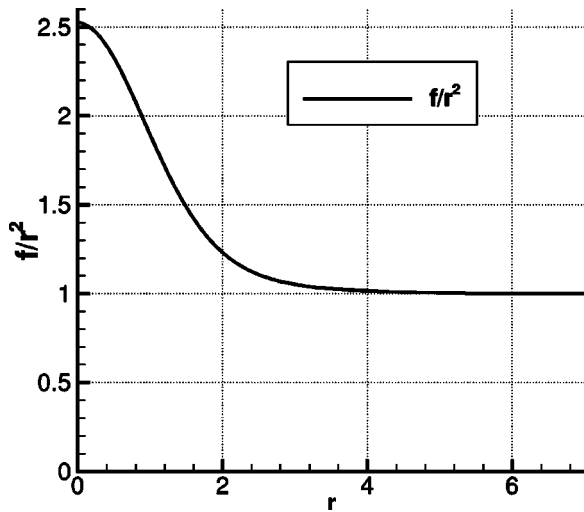


FIG. 1.  $f(r)/r^2$  function.

$$\mathbf{u}_0(r) = [0, r\Omega(r), 0], \tag{2}$$

$$\mathbf{u}_1(r, \theta) = [f/r \sin 2\theta, 1/2 df/dr \cos 2\theta, 0], \tag{3}$$

$\mathbf{u}_0(r)$  represents the velocity field associated with the axisymmetrical vortex,  $\Omega(r)$  designating the angular rotation. For a Lamb–Oseen vortex

$$\Omega(r) = \frac{1 - \exp(-r^2)}{r^2}. \tag{4}$$

The velocity field  $\mathbf{u}_1(r, \theta)$  at order  $\epsilon$  is a straining field whose stretching direction lies along  $\theta = \pi/4$  and whose direction of contraction is along  $\theta = -\pi/4$ . This field depends on the function  $f(r)$  which is determined so as to obtain a steady 2D basic flow—the vortex adapts to the presence of the external straining field. Following Moore and Saffman.<sup>8</sup>

$$\frac{d^2 f}{dr^2} + \frac{1}{r} \frac{df}{dr} - \left( \frac{3d\Omega/dr + rd^2\Omega/dr^2}{r\Omega} + \frac{4}{r^2} \right) f = 0. \tag{5}$$

We impose the following normalization condition:  $f(r)/r^2 \rightarrow 1$  at infinity. Figure 1 shows the numerically obtained function  $f(r)/r^2$ . This result has already been given by Eloy and Le Dizès<sup>10</sup> and shows that the Lamb–Oseen vortex is strained 2.5 times more in its center than in the outer regions. This value has to be compared with the one corresponding to a strained Rankine vortex, for which Moore and Saffman<sup>3</sup> obtained the value of 2.

- (2) The second one consists in a 3D perturbation superposed to this flow. The terms in  $\alpha^i$ , i.e.,  $\mathbf{u}_{01}$ ,  $\mathbf{u}_{02}$ , and so on, describe the weakly nonlinear dynamics of Kelvin waves. The results obtained by Greenspan<sup>25</sup> for a bounded flow in rigid rotation suggests that we will be getting a stable phase dynamics here. The terms in  $\epsilon^i \alpha^j$ , like  $\mathbf{u}_{11}$  or  $\mathbf{u}_{12}$ , describe the couplings that may exist between the straining field and the Kelvin waves. For example, the Widnall instability is obtained at order  $\epsilon\alpha$ . As shown by Waleffe,<sup>19</sup> an axisymmetric mean flow is generated at order  $\alpha^2$  as the instability develops. This mean flow allows the energy of the total flow to be conserved at order  $\epsilon = \alpha^2$ , and is determined at order  $\epsilon\alpha^2$  through a compatibility condition.

### III. THE AMPLITUDE EQUATIONS

We will now proceed along the guidelines given in the preceding section. Here, we give the equations obtained at order  $\epsilon^0 \alpha^1$  which determine  $\mathbf{u}_{01}$ . We will restrict this study to a particular combination of Kelvin waves for  $\mathbf{u}_{01}$ , that is two stationary Kelvin waves with the same axial wave number  $k$ , and with azimuthal wave numbers  $-1$  and  $+1$ . The complex amplitudes of these Kelvin waves are  $A$  and  $B$ . The amplitude equations governing  $A$  and  $B$  are given in Sec. III B, the details of the analysis yielding these equations being postponed to Appendix A.

#### A. Order $\epsilon^0 \alpha^1$

At order  $\epsilon^0 \alpha^1$ , we obtain the following homogeneous linear equation:

$$\partial_t \mathbf{u}_{01} + \mathcal{M} \mathbf{u}_{01} + \nabla p_{01} = 0, \tag{6}$$

$$\text{div} \mathbf{u}_{01} = 0, \tag{7}$$

in which  $\mathcal{M}$  is the matrix

$$\mathcal{M} = \begin{pmatrix} \Omega \partial_\theta & -2\Omega & 0 \\ 2\Omega + rd\Omega/dr & \Omega \partial_\theta & 0 \\ 0 & 0 & \Omega \partial_\theta \end{pmatrix}, \tag{8}$$

$\nabla$  is the gradient operator,  $\nabla \mathbf{u} = (\partial_r u, 1/r \partial_\theta v, \partial_z w)$ , and  $\text{div}$  is the divergence operator,  $\text{div} \mathbf{u} = u/r + \partial_r u + 1/r \partial_\theta v + \partial_z w$ . The following boundary conditions are considered:  $\mathbf{u}_{01} \rightarrow 0$  when  $r \rightarrow \infty$  and  $\mathbf{u}_{01}$  bounded when  $r \rightarrow 0$ . The solutions to these equations are the Kelvin waves. Instability may arise when  $\mathbf{u}_{01}$  is compound of two Kelvin waves with the same axial wave number and frequency but whose azimuthal wave numbers differ by two. In the case of a Rankine vortex, Tsai and Widnall<sup>9</sup> showed that maximum instability is obtained in the case where the Kelvin waves are stationary and the azimuthal wave numbers equal to  $-1$  and  $+1$ . In the following, we only consider this latter case, so that:

$$\mathbf{u}_{01}(r, \theta, z, t) = A e^{-i\theta} e^{ikz} \mathbf{u}_A(r) + B e^{+i\theta} e^{ikz} \mathbf{u}_B(r) + \text{c.c.}, \tag{9}$$

in which c.c. designates the complex conjugate.  $A$  and  $B$  are the complex amplitudes of the two Kelvin waves, while  $\mathbf{u}_A$  and  $\mathbf{u}_B$  are their radial structures. It can easily be shown<sup>8</sup> that  $\mathbf{u}_A$  and  $\mathbf{u}_B$  have a structure of the type  $(iu, v, w)$  with

$$\mathbf{u}_A = (iu_A, v_A, w_A), \quad \mathbf{u}_B = (-iu_A, v_A, -w_A), \tag{10}$$

where  $u_A$ ,  $v_A$ ,  $w_A$  are real functions.  $\mathbf{u}_A$  is determined through

$$\mathcal{M}_{-1} \mathbf{u}_A + \nabla_{-1,k} p_A = 0, \tag{11}$$

$$\text{div}_{-1,k} \mathbf{u}_A = 0, \tag{12}$$

where  $\mathcal{M}_m$ ,  $\nabla_{m,k}$  and  $\text{div}_{m,k}$  are the same operators as before except that the derivatives  $\partial_\theta$  and  $\partial_z$  are replaced by  $im$  and  $ik$ . The same boundary conditions as those given above are considered:  $\mathbf{u}_A \rightarrow 0$  when  $r \rightarrow \infty$  and  $\mathbf{u}_A$  bounded when  $r \rightarrow 0$ . This equation has solutions only for specific values of  $k$ . These solutions correspond to stationary Kelvin waves with  $m = -1$ . In agreement with the results found by Eloy and Le

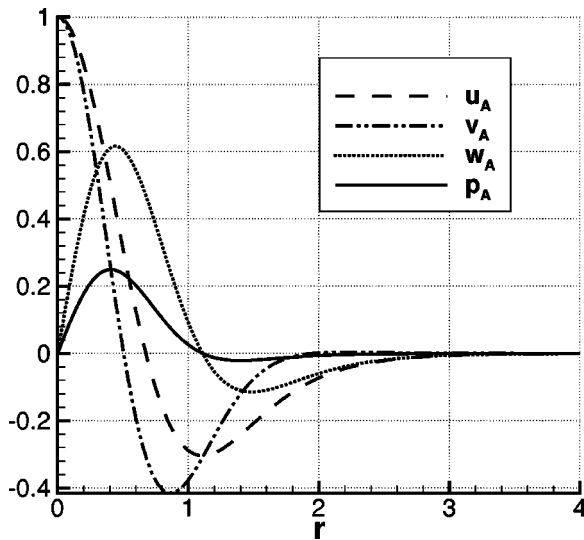


FIG. 2. Kelvin wave  $e^{-i\theta}e^{ikz}\mathbf{u}_A(r)$ . Case  $k=2.261$ .

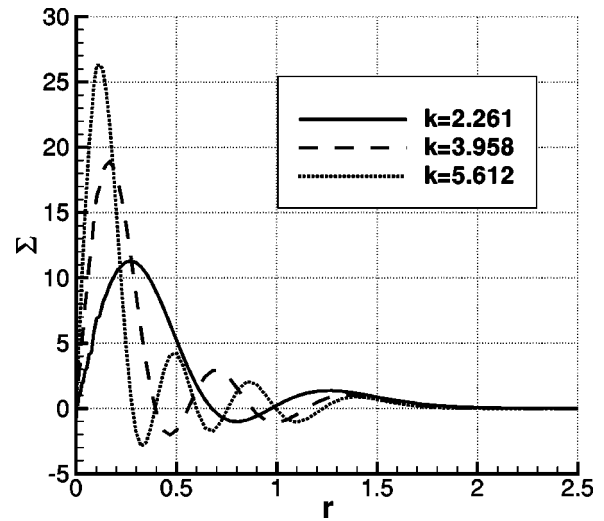


FIG. 3. Created mean flow  $\Sigma(r)$ . Case  $k=2.261, 3.958, 5.612$ .

Dizès,<sup>10</sup> the first three occurrences are  $k=2.261$ ,  $k=3.958$ , and  $k=5.612$ . The radial structure of the three velocity components of  $\mathbf{u}_A$  as well as the corresponding pressure field are given in Fig. 2 in the case  $k=2.261$ . The numerical method used to obtain these results is described in Appendix B.

**B. Final amplitude equations**

The details concerning the rest of the weakly nonlinear analysis are postponed to Appendix A. Here we recall the final result, which consists in three amplitude equations given in (A56)–(A58)

$$\frac{dA}{dt} = +i\epsilon aB - i\epsilon A(b|A|^2 + c|B|^2 + dC), \tag{13}$$

$$\frac{dB}{dt} = -i\epsilon aA + i\epsilon B(c|A|^2 + b|B|^2 + dC), \tag{14}$$

$$\frac{dC}{dt} = +i\epsilon(A\bar{B} - \bar{A}B), \tag{15}$$

where the bar stands for the conjugate. The various constants  $a, b, c, d$  entering in these equations are given in Table I in the cases  $k=2.261, 3.958, 5.612$ .  $A$  and  $B$  are the complex amplitudes of the two stationary Kelvin waves introduced above.  $C$  is the amplitude of the axisymmetrical mean flow generated at order  $\epsilon$  as a result of the instability mechanism. This mean flow is characterized by an azimuthal velocity  $\Sigma(r)$ , which is represented in Fig. 3 in the case  $k=2.261$ ,

$3.958, 5.612$ . Physically, it represents a deceleration of the Lamb–Oseen vortex, due to the growing instability which draws its energy from the basic flow.

**IV. ANALYSIS AND INTERPRETATION OF THE AMPLITUDE EQUATIONS**

**A. Structure of the amplitude equations**

The structure of the amplitude equations [Eqs. (13)–(15)] is the same as that found in Waleffe.<sup>19</sup> In order to recover the structure obtained on grounds of symmetry by Guckenheimer and Mahalov<sup>22</sup> and Knobloch *et al.*,<sup>23</sup> we eliminate the amplitude  $C$  using the energy conservation:  $|A|^2 + |B|^2 + 2aC = E_0$  [Eq. (A61)] and make the variable changes:  $z_1 = A$  and  $z_2 = \bar{B}$ , so as to obtain

$$\frac{dz_1}{dt} = -i\epsilon d'z_1 + i\epsilon a z_2 + i\epsilon z_1(b'|z_1|^2 + c'|z_2|^2), \tag{16}$$

$$\frac{dz_2}{dt} = -i\epsilon d'z_2 + i\epsilon a z_1 + i\epsilon z_2(c'|z_1|^2 + b'|z_2|^2), \tag{17}$$

where  $b' = d/2a - b$ ,  $c' = d/2a - c$ , and  $d' = E_0 d/2a$ . As done in Knobloch *et al.*,<sup>23</sup> we now consider the Hamiltonian structure of this system. The Hamiltonian structure we use is the standard one obtained by taking the real and imaginary part of  $z_i$  as conjugate variables. For example, we write  $z_1 = q_1 + ip_1$  and require  $dq_1/dt = \partial H/\partial p_1$  and  $dp_1/dt = -\partial H/\partial q_1$ . The Hamiltonian related to the above system is:

TABLE I. Values of the different constants  $a, b, c$ , and  $d$  (columns 2, 3, 4, and 5) entering into the amplitude equations. Columns 6 and 7 indicate the theoretically equal values of  $\langle \mathbf{u}_0, \mathbf{t} \rangle$  and  $2a\langle \mathbf{u}_A, \mathbf{u}_A \rangle$ . The phase shift due to the mean field  $D_{MF} = d/a^2$  and that due to the nonlinearities  $D_{NL} = (b+c)/a$  are given in columns 8 and 9. The differential phase shift  $D = D_{MF} - D_{NL}$  between the two values is given in column 10.

$k$	$a$	$b$	$c$	$d$	$\langle \mathbf{u}_0, \mathbf{t} \rangle$	$2a\langle \mathbf{u}_A, \mathbf{u}_A \rangle$	$D_{MF}$	$D_{NL}$	$D$
2.261	1.379	0.151	0.370	2.34	0.9582	0.9582	1.23	0.378	0.852
3.958	1.389	0.111	0.648	4.93	0.5775	0.5775	2.56	0.546	2.01
5.612	1.391	0.0869	1.01	7.64	0.4130	0.4130	3.95	0.789	3.16

$$H(z_1, z_2) = -\epsilon a \operatorname{Re}(z_1 z_2) + \frac{1}{2} \epsilon d' (|z_1|^2 + |z_2|^2) - \frac{1}{4} \epsilon b' (|z_1|^4 + |z_2|^4) - \frac{1}{2} \epsilon c' |z_1|^2 |z_2|^2, \quad (18)$$

where  $\operatorname{Re}$  designates the real part of a complex number. The quantity  $H$  is an integral of Eqs. (16) and (17).

Now, introducing the quantity

$$J(z_1, z_2) = |z_1|^2 - |z_2|^2, \quad (19)$$

one can readily check that  $J$  is also a conserved quantity. As a conclusion, the above system displays two conserved quantities, the Hamiltonian  $H$  and the quantity  $J$ .

### B. Subspace $B = \bar{A}$

In the remainder of this study, we will be restricting ourselves to the case where  $B = \bar{A}$ , for which Eq. (14) is equivalent to Eq. (13). This subspace is characterized by  $J = 0$ . Equations (13) and (15) become

$$\frac{dA}{dt} = i\epsilon a \bar{A} - i\epsilon A [(b+c)|A|^2 + dC], \quad (20)$$

$$\frac{dC}{dt} = i\epsilon (A^2 - \bar{A}^2). \quad (21)$$

If  $A = |A|e^{i\phi}$ , the leading-order term of the 3D perturbation field is  $\sqrt{\epsilon} \mathbf{u}_{01}$  where:

$$\mathbf{u}_{01} = |A|e^{i\phi} e^{-i\theta} e^{ikz} \mathbf{u}_A(r) + |A|e^{-i\phi} e^{i\theta} e^{ikz} \mathbf{u}_B(r) + \text{c.c.} \quad (22)$$

By determining this term explicitly and taking its curl, we get the following expressions for the radial vorticity  $\omega_{01}^r$ , the ortho-radial vorticity  $\omega_{01}^\theta$  and the axial vorticity  $\omega_{01}^z$  of the perturbation field:

$$\omega_{01}^r(r, \theta, z, t) = -4|A| \sin kz \cos(\theta - \phi) \omega_A^r(r), \quad (23)$$

$$\omega_{01}^\theta(r, \theta, z, t) = +4|A| \sin kz \sin(\theta - \phi) \omega_A^\theta(r), \quad (24)$$

$$\omega_{01}^z(r, \theta, z, t) = +4|A| \cos kz \cos(\theta - \phi) \omega_A^z(r), \quad (25)$$

where  $\omega_A^r$ ,  $\omega_A^\theta$ , and  $\omega_A^z$  designate the radial structure of the vorticity field related to the Kelvin wave  $A$

$$|A|e^{i\phi} e^{-i\theta} e^{ikz} \omega_A(r) = |A|e^{i\phi} e^{-i\theta} e^{ikz} [i\omega_A^r(r), \omega_A^\theta(r), \omega_A^z(r)]. \quad (26)$$

The vorticity field of the 3D perturbation is shown in Fig. 4 for  $\phi = \pi/6$  and  $kz = 3\pi/4$ . If  $\phi = \pi/4$ , i.e., if the horizontal vorticity lies in the stretching direction of the basic flow, then the structure of the perturbation is analogous to the structure of the elliptical eigenmode given by Waleffe<sup>13</sup> in the case of an unbounded elliptical flow. This perturbation field induces a displacement of the vortex center, as shown by Leweke and Williamson.<sup>1</sup> By defining the vortex center  $(x_c, y_c)$  by the zero velocity point or the minimum pressure point (it can be shown that these two definitions give the same center), we obtain

$$x_c = -4\sqrt{\epsilon}|A| \cos kz \cos \phi, \quad (27)$$

$$y_c = -4\sqrt{\epsilon}|A| \cos kz \sin \phi. \quad (28)$$

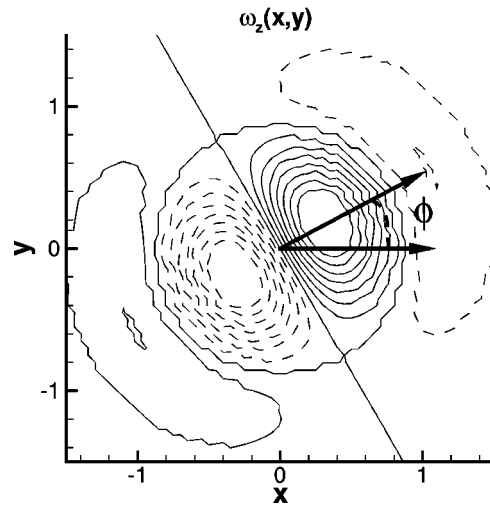
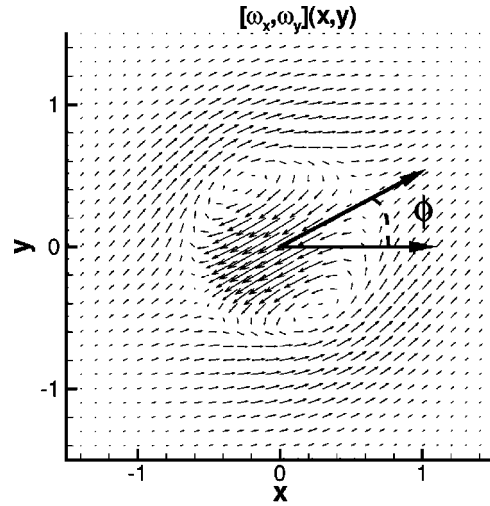


FIG. 4. Vorticity structure of the perturbation  $\mathbf{u}_{01}$  characterized by the angle  $\phi$ . Case  $k = 2.261$ .

We have used here the fact that we chose  $u_A(0) = (dp_A/dr)(0) = 1$ . The physical interpretation of  $|A|$  and of  $\phi$  is, therefore, clear: The perturbation  $\mathbf{u}_{01}$  corresponds to a vortex oscillation in a plane inclined at an angle  $\phi$  with respect to the horizontal, and whose amplitude is proportional to  $|A|$ .

### C. Weakly nonlinear saturation of the elliptic instability

By considering  $C' = aC$  and  $\tau = \epsilon at$ , Eqs. (20) and (21) become

$$\frac{dA}{d\tau} = i\bar{A} - iA(D_{NL}|A|^2 + D_{MF}C'), \quad (29)$$

$$\frac{dC'}{d\tau} = i(A^2 - \bar{A}^2), \quad (30)$$

in which

$$D_{NL} = (b+c)/a, \quad (31)$$

$$D_{MF} = d/a^2. \quad (32)$$

In polar coordinates,  $A = |A|e^{i\phi}$ , these equations are expressed as

$$\frac{d|A|}{d\tau} = |A| \sin 2\phi, \tag{33}$$

$$\frac{d\phi}{d\tau} = \cos 2\phi - D_{NL}|A|^2 - D_{MF}C', \tag{34}$$

$$\frac{dC'}{d\tau} = -2|A|^2 \sin 2\phi. \tag{35}$$

The constants  $D_{NL}$  and  $D_{MF}$  are given in Table I. We now have a clear view of the physical mechanisms at play in the amplitude equations [Eqs. (33) and (34)].

The linear short-wave instability is obtained when  $|A| \ll 1$ . We then consider only the two terms  $|A| \sin 2\phi$  and  $\cos 2\phi$ . The system is linearly unstable: The unstable direction,  $\phi = \pi/4$  corresponds to a perturbation whose vorticity in the  $(x, y)$  plane is aligned with the stretching direction of the basic flow. The direction  $\phi = -\pi/4$ , on the other hand, is stable: The horizontal vorticity of the perturbation is aligned with the direction of contraction of the straining field. Parallel to this amplification–attenuation of the vorticity in the  $(x, y)$  plane, the vortex center is subject to a sinusoidal deformation in a plane making an angle  $\phi$  with the horizontal. The amplitude of these oscillations increases–decreases exponentially in a plane set in the directions  $\phi = \pm \pi/4$ .

The nonlinear effects are felt when the order of magnitude of  $|A|$  becomes unity. Only Eq. (34) governing the phase of the perturbation is affected by these nonlinear corrections, and not the equation governing the amplitude (33). Equation (34) shows that the nonlinearities (term in  $D_{NL}$ ) as well as the mean field (term in  $D_{MF}$ ) will phase-shift the system and may prompt the perturbation to leave the unstable direction.

The nonlinearities and the mean field shift the perturbation phase in opposite directions. Indeed, the system of Eqs. (29) and (30) conserves the energy:  $|A|^2 + C' = E_0$ . Here  $E_0 = |A_0|^2$  since the energy of the mean field at order  $\alpha^2 = \epsilon$  is supposed to be zero at time  $t = 0$ :  $C'_0 = 0$ . It follows:

$$\frac{dA}{d\tau} = +i\bar{A} + iA(D|A|^2 - D_0), \tag{36}$$

in which

$$D = D_{MF} - D_{NL}, \tag{37}$$

$$D_0 = D_{MF}|A_0|^2. \tag{38}$$

In polar coordinates,  $A = |A|e^{i\phi}$

$$\frac{d|A|}{d\tau} = |A| \sin(2\phi), \tag{39}$$

$$\frac{d\phi}{d\tau} = \cos(2\phi) + D|A|^2 - D_0. \tag{40}$$

The total phase shift is compound of two terms,  $D|A|^2$  and  $-D_0$ . The latter term is a measure of the amplitude of the initial condition whereas the former term displays a constant  $D$  which is the differential phase shift between the two posi-

tive terms  $D_{MF}$  and  $D_{NL}$ . The effect of the mean field ( $D_{MF}$  term) is, therefore, opposed to the effect of the nonlinearities ( $D_{NL}$  term). As the results of Table I show, it is the phase shift due to the mean field that prevails over that due to the nonlinearities ( $D_{MF} > D_{NL}$ ). The value of  $D$  is important in the dynamics of the system: The larger  $D$ , the greater the phase shift when  $|A|$  becomes large, and, therefore, the faster the perturbation will leave its direction of maximum instability  $\phi = \pi/4$ . A limiting case can be imagined where  $D = 0$ , and for which the phase shift of the mean field and that of the nonlinearities cancel out exactly. The system is then unstable at this order and the weakly nonlinear expansion would have to be continued at the next order in order to conclude. But  $D$  is never zero, and so this case does not occur.

Let us now make the variable changes  $A' = \sqrt{D}A$  and  $C'' = DC' = aDC$ . We then get

$$\frac{dA'}{d\tau} = +i\bar{A}' + iA'(|A'|^2 - D_0), \tag{41}$$

$$|A'|^2 + C'' = |A'_0|^2, \tag{42}$$

in which  $D_0 = D_{MF}|A'_0|^2/D$ . Guckenheimer and Mahalov,<sup>22</sup> who obtained the Hamiltonian normal form (41) on grounds of symmetry, already studied its dynamics in the full phase space. Note that some of the results were first described by Waleffe.<sup>19</sup> Here we briefly recall the principle ones. In polar coordinates,  $A' = |A'|e^{i\phi}$ , the above system yields

$$\frac{d|A'|}{d\tau} = |A'| \sin(2\phi), \tag{43}$$

$$\frac{d\phi}{d\tau} = \cos(2\phi) + |A'|^2 - D_0. \tag{44}$$

Depending on the amplitude of the initial conditions, we obtain the following structures:

- (i) If  $0 \leq D_0 < 1$ , there exists an unstable fixed point at  $A' = 0$  where the amplification rate is equal to  $\sqrt{1 - D_0^2}$ . This point corresponds to the linear short-wave instability. Two fixed stable points are located at  $A' = \pm i\sqrt{1 + D_0}$  and correspond to a perturbation whose horizontal vorticity is aligned with the  $e_y$  direction.
- (ii) If  $D_0 > 1$ , the fixed point at  $A' = 0$  becomes stable. This means that the initial amplitude of the perturbation is sufficiently large to induce a phase shift which prevents the occurrence of the short-wave instability. Two unstable fixed points appear at  $A' = \pm \sqrt{D_0 - 1}$ . The horizontal vorticity of the perturbation is aligned in these two cases with the  $Ox$  direction. The amplification rate is equal to  $2\sqrt{D_0 - 1}$ . The two fixed stable points in  $A' = \pm i\sqrt{1 + D_0}$  still exist.

From now on, we restrict ourselves to the case  $k = 2.261$ , for which  $D_{MF} = 1.23$ ,  $D_{NL} = 0.378$ , and  $D = 0.852$ . In the case  $D_0 = 0.1$ , which corresponds to  $|A'_0| = 0.26$ , Fig. 5 represents two trajectories corresponding to  $\phi_0 = 0, -\pi/2$  in the phase space, which is three-dimensional here. It can be seen that the perturbation first gains energy (instability phase), drawing it from the vortex ( $C''$  becomes negative).

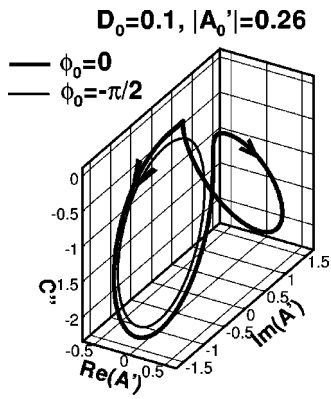


FIG. 5. Dynamics in the phase space. Case  $k=2.261$ .

Then, as the amplitude of the unstable mode increases, the perturbation phase is shifted by the  $|A'|^2$  term. The amplitude of the unstable mode then saturates and the angle  $\phi$  sets in the direction of contraction of the straining field  $\phi = -\pi/4$ .

The perturbation then returns its energy to the basic flow, and attenuates until a new linear regime is reached in which the phase shift terms are negligible. The vortex may even gain energy ( $C'' > 0$ ), but this phase is transitory because the linear process will re-select an unstable mode, which will increase, and so forth. A similar discussion is to be found in the Ph.D. thesis of Waleffe<sup>19</sup> which deals with the weakly nonlinear development of elliptic instability in the case of a bounded strained uniform vortex. In particular, the phenomenology with the nonlinear phase shifting has already been given there.

From now on, instead of representing the trajectories in the full 3D phase space, we will only give their projection on a plane  $C'' = \text{cst}$ . Equation (42) expressing energy conservation will allow us to determine  $C''$  as a function of  $A'$  at any time. The cases  $D_0 = 0.1, 0.75, 1, 2, 10$  are analyzed in Fig. 6. Each plot shows the projection of the trajectories on the plane  $C'' = \text{cst}$ . The circle describes the allowable initial conditions in this plane. These are determined by the relation

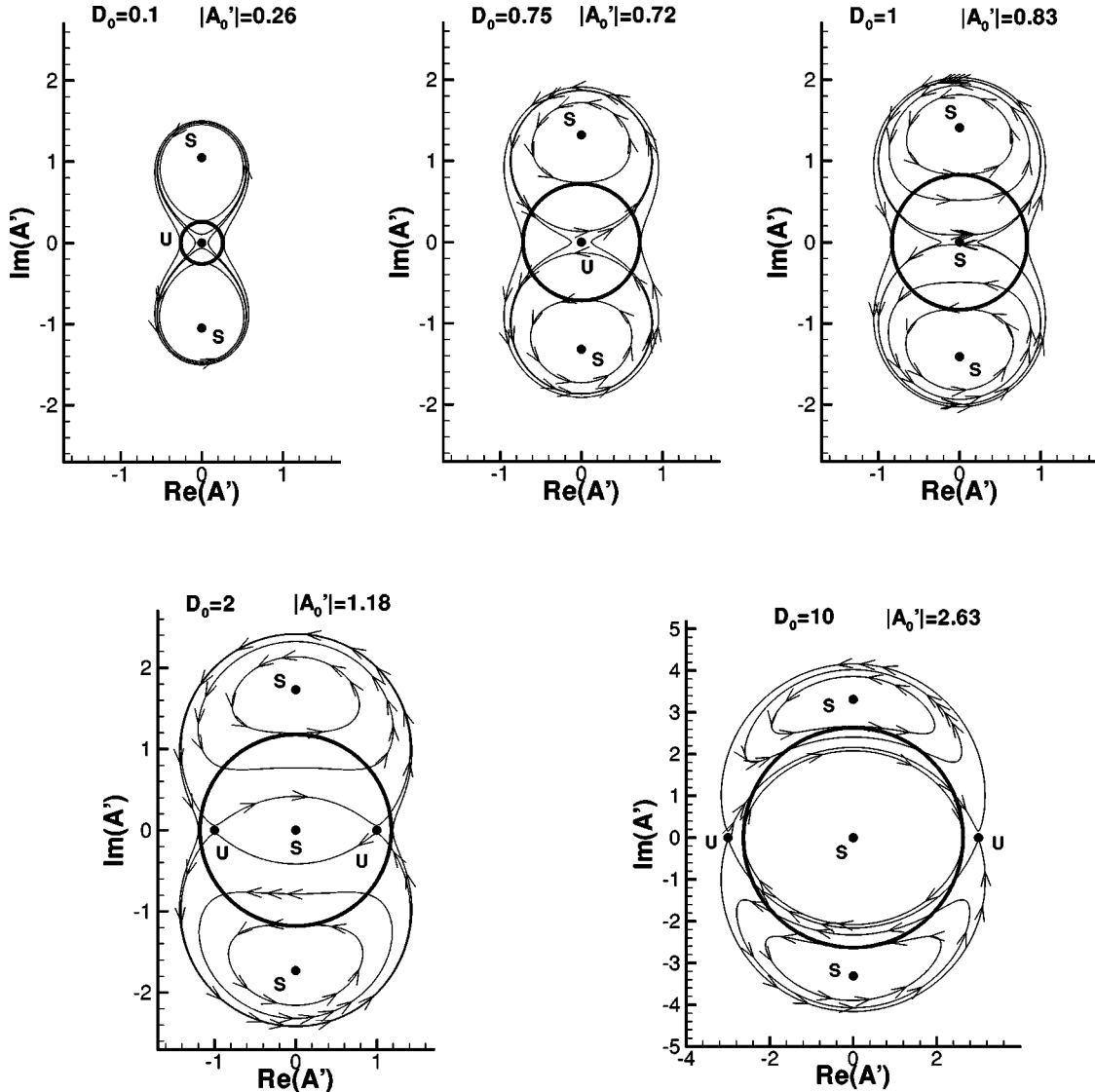


FIG. 6. Trajectories in the phase space projected on a plane  $C'' = \text{cte}$  in the cases  $D_0 = 0.1, 0.75, 1, 2, 10$ . The circle in each figure represents the initial allowable conditions  $A'_0$ . Case  $k=2.261$ .

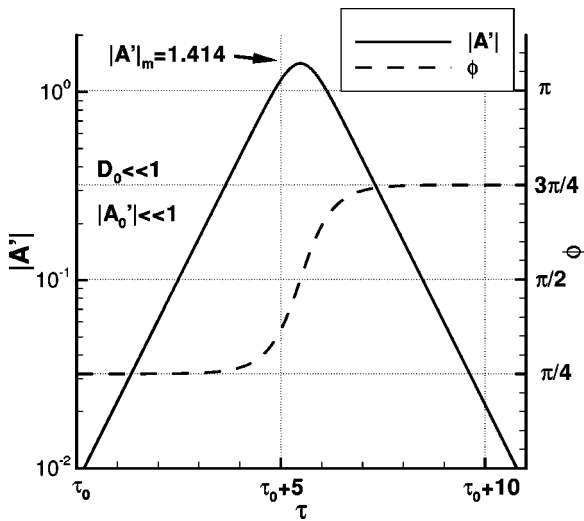


FIG. 7. Saturation of the Widnall instability in the case  $D_0 \ll 1$ .

$D_0 = D_{MF}|A'_0|^2/D$  that sets  $|A'_0|$  as a function of  $D_0$ . This restriction stems from the fact that we are restricting ourselves here for the initial conditions to the plane  $C''=0$ . In other words, at the time origin, the mean field consists exclusively of the Lamb–Oseen vortex, the mean field at order  $\alpha^2$  being zero at this time. The fixed points determined above are also indicated in each figure. These are marked by the letter *S* if the fixed point is stable, and the letter *U* if it is not. We then represent various trajectories whose origins are always located on the previously mentioned circle. We see that we obtain a stable system for any initial condition, i.e., all trajectories are constrained to a bounded domain in the phase space. The phase-plane diagrams presented in Fig. 6 are similar to those given in Guckenheimer and Mahalov<sup>22</sup> and Knobloch *et al.*<sup>23</sup>

**D. Case for which  $D_0 \ll 1$**

The  $D_0 \ll 1$  case is of special importance because it corresponds to the physical situation where the emerging mode is completely determined by the linear instability. Physically, this corresponds to the case of a perturbation of weak initial intensity, amplified linearly by the system. The emerging mode is then purely in the  $\phi = \pi/4$  direction. Figure 7 describes this situation, graphing the amplitude  $|A'|$  and the phase  $\phi$  as a function of time  $\tau$ . This figure is valid for all cases  $k = 2.261, 3.958, 5.612$ , because the condition  $D_0 \ll 1$  does not allow us to differentiate these cases. It is only through the change of variable  $A' = \sqrt{D}A$  that the differentiation reappears, because the constants  $D$  are different in each case. The angle  $\phi$  is initially equal to  $\pi/4$ , and the amplitude  $|A'_0|$  equal to  $10^{-2}$ . These values are not restrictive because we know that any initial condition such that  $D_0 \ll 1$  will go through this state. The figure shows that the amplification rate remains nearly the same until saturation. This is due to the fact that, in Eq. (43), there is no nonlinear correction term. The nonlinearities act exclusively on the phase of the mode. The transition from the direction of stretch of the basic flow  $\phi = \pi/4$  to that of its contraction occurs very quickly in one or two times  $\tau$ . This means that

TABLE II. Saturation amplitudes  $\Delta/b$  of the short-wave instability for a few characteristic aspect ratios  $a/b$ .

$a/b$	$ka = 2.261$	$ka = 3.958$	$ka = 5.612$
0.01	0.000 61	0.0004	0.000 32
0.1	0.061	0.04	0.032
0.15	0.14	0.09	0.072
0.20	0.24	0.16	0.13
0.25	0.38	0.25	0.20
0.3	0.55	0.36	0.29

the oscillations increase exponentially in a plane inclined at an angle  $\phi = \pi/4$  and that, just before saturation this plane turns rapidly, passes through the vertical direction, and settles in the  $3\pi/4$  direction. The amplitude of the oscillations then decreases exponentially again.

The maximum amplitude achieved in Fig. 7 is  $|A'|_m = 1.414$ . Now, the maximum amplitude of the vortex oscillations over time is equal to:  $\Delta = \max_{\tau} \max_z \sqrt{x_c^2 + y_c^2}$  where  $x_c$  and  $y_c$  are given in (27) and (28). Thus

$$\Delta = 4 \sqrt{\epsilon} |A|_m = 4 \sqrt{\epsilon} |A'|_m / \sqrt{D}. \tag{45}$$

**V. APPLICATION OF THE RESULTS TO THE CASE OF A VORTEX PAIR**

We will now consider the case of a pair of counter-rotating Lamb–Oseen vortices of intensity  $\pm\Gamma$ , of radius  $a$  and separated by the distance  $b$ . In Eq. (45),  $\epsilon$  and  $\Delta$  were nondimensional quantities (up to now, distances were nondimensionalized by  $a$  and times by  $2\pi a^2/\Gamma$ ). In order to come back to dimensional variables,  $\Delta$  has to be replaced by  $\Delta/a$  and  $\epsilon$  by  $a^2/b^2$ . Considering the fact that  $|A'|_m = 1.414$ , we obtain

$$\frac{\Delta}{b} = 5.7/\sqrt{D} \frac{a^2}{b^2}. \tag{46}$$

$D$  is the differential phase shift, the value of which is given in Table I in the cases  $ka = 2.261, 3.958, 5.612$ . Evaluating these various terms yields

$$\frac{\Delta}{b} = 6.1 \frac{a^2}{b^2} \text{ for } ka = 2.261, \tag{47}$$

$$\frac{\Delta}{b} = 4.0 \frac{a^2}{b^2} \text{ for } ka = 3.958, \tag{48}$$

$$\frac{\Delta}{b} = 3.2 \frac{a^2}{b^2} \text{ for } ka = 5.612. \tag{49}$$

We note that the case  $ka = 2.261$  gives the maximum amplitudes. A few values of the saturation amplitude  $\Delta/b$  are given in Table II for typical aspect ratios in the aeronautical field ( $a/b < 0.1$ ) and in laboratory experiments ( $a/b = 0.2$  for Leweke and Williamson<sup>1</sup>). In the case  $a/b = 0.2$ , the saturation amplitude is  $\Delta/b = 0.24$  for  $ka = 2.261$ . In their experiments, Leweke and Williamson<sup>1</sup> observed vortex displacements compatible with this value. Note that when large amplitude oscillations are obtained, our approach does not include the possible interaction with the other vortex, which may also be subject to strong oscillations. But in the case of

aircraft vortices, the aspect ratios  $a/b$  are much smaller (typically  $a/b < 0.1$ ), so that we can infer that the oscillations due to the considered short-wave instability will saturate at very low amplitude.

### VI. CONCLUSION

In this article, we have achieved a weakly nonlinear analysis of the short-wave instabilities occurring in a strained Lamb–Oseen vortex.

In Sec. III, we gave the amplitude equations which involve two quantities: The complex amplitude  $A = |A|e^{i\phi}$  of the leading-order term of the 3D perturbation and the real amplitude  $C$  of the created mean field at order  $\alpha^2 = \epsilon$ . The flow associated to  $A$  represents a perturbation which induces a vortex oscillation in a plane inclined at an angle  $\phi$ , and whose amplitude is proportional to  $|A|$ . The flow associated to  $C$  constitutes a deceleration of the Lamb–Oseen vortex, due to the growing instability which draws its energy from the basic flow.

In Sec. IV, we have analyzed the dynamics of these amplitude equations. We first retrieved the features of the linear short-wave instabilities, exhibited by Moore and Saffman<sup>8</sup> and Eloy and Le Dizès,<sup>10</sup> i.e., the linear regime selects the particular perturbation  $\phi = \pi/4$ , which corresponds to the stretching direction of the basic flow. The non-linear effects as well as those related to the created mean field at order  $\alpha^2$  are then described. We have shown that these two effects, characterized by the constants  $D_{NL}$  and  $D_{MF}$ , phase shift the perturbation out of the stretching direction  $\phi = \pi/4$  as soon as the amplitude of  $A$  becomes sufficiently large. Their action is antagonistic and the phase shift due to the mean field ( $D_{MF}$  term) is found to be larger than that due to the nonlinearities ( $D_{NL}$  term). The value of the differential phase shift  $D = D_{MF} - D_{NL} > 0$  is, therefore, important in the dynamics of the system, since it characterizes the total effect of the phase shift due both to the nonlinearities and the mean field. The dynamics in the three-dimensional phase space has been studied. It turns out that in all cases the trajectories are constrained to a bounded domain. A detailed analysis of the case for which the amplitude of the initial conditions is very small has been given. Here, the linear regime selects a perturbation whose phase is equal to  $\phi = \pi/4$ . This eigenmode grows exponentially until a critical value of the amplitude is obtained. Then, the nonlinearities and the created mean-field prompt the perturbation to leave the unstable direction, and the phase settles in the  $-\pi/4$  direction, which corresponds to the direc-

tion of contraction of the basic flow. The perturbation then returns its energy to the basic flow, and attenuates until a new linear regime is reached in which the phase shift terms are negligible. The whole process (linear instability, saturation, attenuation) may start again.

In Sec. V, we have applied these results to the case of a vortex pair characterized by the internal radius  $a$  of the vortices and their separation distance  $b$ . We have evaluated the maximum value of the oscillation amplitudes  $\Delta$  as a function of the dipole aspect ratio  $a/b$ . In the case  $ka = 2.261$ , we have shown that  $\Delta/b = 6.1a^2/b^2$ . In the case of Leweke and Williamson’s experiment, for which  $a/b = 0.2$ , our result is in accordance with the observations. In aeronautical situations, which are characterized by smaller values of the dipole aspect ratio, i.e.,  $a/b < 0.1$ , this result also shows that the considered short-wave instability will saturate at very low amplitude.

One has to be cautious, however, in the interpretation of the results presented in this paper. One could conclude that short-wave instabilities do not play a role in the dispersion of aircraft wakes, characterized by very small values of the aspect-ratio  $a/b$ . This strong statement does not follow from the work described in this paper since one has to keep in mind the two following facts. First, the works of Kerswell<sup>20</sup> and Mason and Kerswell<sup>21</sup> suggest that the weakly nonlinear saturated states are themselves unstable and, therefore, fail to represent the outcome of the instability. Second, the technique used in this article limits consideration to local bifurcations of the system whereas global bifurcations do also occur.<sup>24</sup>

### ACKNOWLEDGMENT

The author would like to thank Laurent Jacquin for fruitful discussions on this problem.

### APPENDIX A: THE AMPLITUDE EQUATIONS

#### 1. Order $\epsilon^1 \alpha^1$

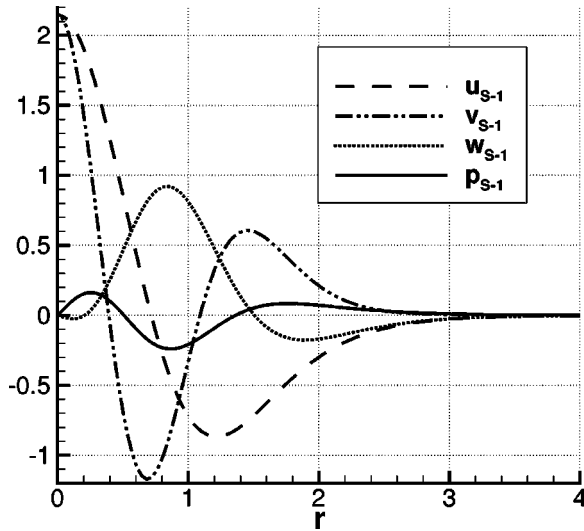
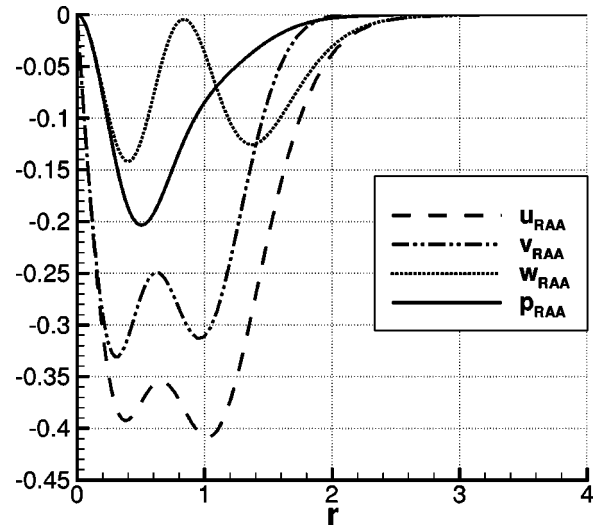
At order  $\epsilon^1 \alpha^1$ , we get the following inhomogeneous linear equation:

$$\partial_t \mathbf{u}_{11} + \mathcal{M} \mathbf{u}_{11} + \nabla p_{11} = e^{2i\theta} \mathcal{N} \mathbf{u}_{01} + e^{-2i\theta} \bar{\mathcal{N}} \bar{\mathbf{u}}_{01}, \tag{A1}$$

$$\text{div } \mathbf{u}_{11} = 0, \tag{A2}$$

where  $\mathcal{N}$  is the matrix

$$\mathcal{N} = \frac{1}{2} \begin{pmatrix} \frac{i}{r} \frac{df}{dr} - \frac{if}{r^2} + \frac{if}{r} \partial_r - \frac{1}{2r} \frac{df}{dr} \partial_\theta & \frac{1}{r} \frac{df}{dr} - \frac{2f}{r^2} & 0 \\ -\frac{1}{2} \frac{d^2f}{dr^2} - \frac{1}{2r} \frac{df}{dr} & -\frac{i}{r} \frac{df}{dr} + \frac{if}{r^2} + \frac{if}{r} \partial_r - \frac{1}{2r} \frac{df}{dr} \partial_\theta & 0 \\ 0 & 0 & \frac{if}{r} \partial_r - \frac{1}{2r} \frac{df}{dr} \partial_\theta \end{pmatrix}, \tag{A3}$$

FIG. 8. Velocity and pressure fields of  $e^{-i\theta}e^{ikz}s_{-1}(r)$ . Case  $k=2.261$ .FIG. 9. Velocity and pressure fields of  $e^{-2i\theta}e^{2ikz}r_{AA}(r)$ . Case  $k=2.261$ .

and  $\bar{\mathcal{N}}$  the conjugate of  $\mathcal{N}$ . Considering Eq. (9), we obtain:

$$\begin{aligned} \partial_t \mathbf{u}_{11} + \mathcal{M} \mathbf{u}_{11} + \nabla p_{11} = & A e^{+i\theta} e^{ikz} \mathcal{N}_{-1} \mathbf{u}_A \\ & + B e^{+3i\theta} e^{ikz} \mathcal{N}_{+1} \mathbf{u}_B \\ & + A e^{-3i\theta} e^{ikz} \bar{\mathcal{N}}_{-1} \mathbf{u}_A \\ & + B e^{-i\theta} e^{ikz} \bar{\mathcal{N}}_{+1} \mathbf{u}_B + \text{c.c.}, \end{aligned} \quad (\text{A4})$$

where  $\mathcal{N}_m$  and  $\bar{\mathcal{N}}_m$  represent the same matrices as  $\mathcal{N}$  and  $\bar{\mathcal{N}}$  except that the terms in  $\partial_\theta$  are replaced by  $im$ .

We then look for  $\mathbf{u}_{11}$  in a separable form:

$$\begin{aligned} \mathbf{u}_{11}(r, \theta, z, t) = & A e^{+i\theta} e^{ikz} \mathbf{s}_{+1}(r) + B e^{+3i\theta} e^{ikz} \mathbf{s}_{+3}(r) \\ & + A e^{-3i\theta} e^{ikz} \mathbf{s}_{-3}(r) + B e^{-i\theta} e^{ikz} \mathbf{s}_{-1}(r) \\ & + \text{c.c.}, \end{aligned} \quad (\text{A5})$$

$\mathbf{s}_{+1}$ ,  $\mathbf{s}_{+3}$ ,  $\mathbf{s}_{-3}$ , and  $\mathbf{s}_{-1}$  are vectors with three components.  $\mathbf{s}_{-1}$  should be defined by

$$\mathcal{M}_{-1} \mathbf{s}_{-1} + \nabla_{-1,k} p_{s-1} = \bar{\mathcal{N}}_1 \mathbf{u}_B, \quad (\text{A6})$$

$$\text{div}_{-1,k} \mathbf{s}_{-1} = 0, \quad (\text{A7})$$

with  $\mathbf{s}_{-1} \rightarrow 0$  when  $r \rightarrow \infty$  and  $\mathbf{s}_{-1}$  bounded when  $r \rightarrow 0$ . But this equation does not admit solutions in general because the Kelvin wave  $\mathbf{u}_A$  is a solution of the corresponding homogeneous equation. A compatibility condition therefore exists for the forcing term in order for Eqs. (A6) and (A7) to have a solution. This compatibility condition requires that the forcing term be orthogonal to  $\mathbf{u}_A$ .

We consider the following scalar product:

$$\langle \mathbf{u}_1, \mathbf{u}_2 \rangle = \int_0^\infty (\bar{u}_1 u_2 + \bar{v}_1 v_2 + \bar{w}_1 w_2) r dr, \quad (\text{A8})$$

and determine the adjoint eigenmode  $\mathbf{u}_A^\perp$  corresponding to  $\mathbf{u}_A$  through

$$\mathcal{M}_{-1}^\perp \mathbf{u}_A^\perp + \nabla_{-1,k} p_A^\perp = 0, \quad (\text{A9})$$

$$\text{div}_{-1,k} \mathbf{u}_A^\perp = 0, \quad (\text{A10})$$

with  $\mathbf{u}_A^\perp \rightarrow 0$  when  $r \rightarrow \infty$  and  $\mathbf{u}_A^\perp$  bounded when  $r \rightarrow 0$ . Here

$$\mathcal{M}_m^\perp = \begin{pmatrix} -im\Omega & 2\Omega + rd\Omega/dr & 0 \\ -2\Omega & -im\Omega & 0 \\ 0 & 0 & -im\Omega \end{pmatrix}. \quad (\text{A11})$$

It can be verified that  $\mathbf{u}_A^\perp$  is of the  $(iu, v, w)$  type

$$\mathbf{u}_A^\perp = (iu_A^\perp, v_A^\perp, w_A^\perp), \quad (\text{A12})$$

where  $u_A^\perp$ ,  $v_A^\perp$ ,  $w_A^\perp$  are real functions.

We then make the amplitudes  $A$  and  $B$  depend on a slow time scale based on  $1/\epsilon$  so that a new term  $-(1/\epsilon)(1/B)(dA/dt)\mathbf{u}_A$  appears on the right-hand-side of Eq. (A6). We then determine  $dA/dt$  so as to ensure the compatibility condition. Hence

$$\frac{dA}{dt} = i\epsilon a_A B, \quad (\text{A13})$$

$$ia_A = \frac{\langle \mathbf{u}_A^\perp, \bar{\mathcal{N}}_1 \mathbf{u}_B \rangle}{\langle \mathbf{u}_A^\perp, \mathbf{u}_A \rangle}, \quad (\text{A14})$$

$\mathbf{s}_{-1}$  will then be a solution of

$$\mathcal{M}_{-1} \mathbf{s}_{-1} + \nabla_{-1,k} p_{s-1} = \bar{\mathcal{N}}_1 \mathbf{u}_B - \frac{\langle \mathbf{u}_A^\perp, \bar{\mathcal{N}}_1 \mathbf{u}_B \rangle}{\langle \mathbf{u}_A^\perp, \mathbf{u}_A \rangle} \mathbf{u}_A, \quad (\text{A15})$$

$$\text{div}_{-1,k} \mathbf{s}_{-1} = 0. \quad (\text{A16})$$

The general solution of this equation is equal to a particular solution, to which a solution of the homogeneous equation,  $\lambda \mathbf{u}_A$  where  $\lambda$  is arbitrary, must be added. This is the Fredholm alternative.

An analogous treatment can be applied for  $\mathbf{s}_{+1}$  and it can be verified that the compatibility condition is expressed here by

$$\frac{dB}{dt} = -i\epsilon a_B A, \quad (\text{A17})$$

$$ia_B = - \frac{\langle \mathbf{u}_B^\perp, \mathcal{N}_{-1} \mathbf{u}_A \rangle}{\langle \mathbf{u}_B^\perp, \mathbf{u}_B \rangle}, \tag{A18}$$

where  $\mathbf{u}_B^\perp$  is defined through

$$\mathcal{M}_{+1}^\perp \mathbf{u}_B^\perp + \nabla_{+1,k} p_B^\perp = 0, \tag{A19}$$

$$\text{div}_{+1,k} \mathbf{u}_B^\perp = 0. \tag{A20}$$

It can be verified<sup>8</sup> that the following symmetry holds:

$$\mathbf{u}_B^\perp = (-iu_A^\perp, v_A^\perp, -w_A^\perp), \tag{A21}$$

$a_A$  and  $a_B$  are two real constants which are equal. This is due to the fact that the matrices  $\mathcal{N}_{-1}$  and  $\bar{\mathcal{N}}_{+1}$  have diagonals with purely imaginary coefficients, and purely real terms off the diagonal. Their action on vectors of structure  $(iu, v, w)$  therefore, yields vectors of structure  $(u, iv, iw)$ . Now, considering the explicit expressions of  $\mathbf{u}_A$ ,  $\mathbf{u}_B$ ,  $\mathbf{u}_A^\perp$ , and  $\mathbf{u}_B^\perp$  given in (10), (A12), and (A21), the evaluation of the scalar products involved in (A14) and (A18) then shows that  $a_A$  and  $a_B$  are reals and that  $a_A = a_B = a$ . Also, a careful check shows that the following expressions hold for  $\mathbf{s}_{-1}$  and  $\mathbf{s}_{+1}$ :

$$\begin{aligned} \mathbf{s}_{-1} &= (iu_{s-1}, v_{s-1}, w_{s-1}), \\ \mathbf{s}_{+1} &= (-iu_{s-1}, v_{s-1}, -w_{s-1}), \end{aligned} \tag{A22}$$

where all the introduced functions are real. These functions as well as the corresponding pressure field are displayed in Fig. 8. The constant  $a$  is given in Table I in the cases  $k = 2.261, 3.958, 5.612$ . The numerical values are the same as those given by Eloy and Le Dizès.<sup>10</sup>

## 2. Order $\epsilon^0 \alpha^2$

At order  $\epsilon^0 \alpha^2$ , we obtain the following inhomogeneous linear equation:

$$\partial_t \mathbf{u}_{02} + \mathcal{M} \mathbf{u}_{02} + \nabla p_{02} = \{\mathbf{u}_{01}, \mathbf{u}_{01}\}, \tag{A23}$$

$$\text{div} \mathbf{u}_{02} = 0, \tag{A24}$$

where  $\{\mathbf{u}_1, \mathbf{u}_2\}$  designates the term  $-\mathbf{u}_1 \cdot \nabla \mathbf{u}_2$

$$\{\mathbf{u}_1, \mathbf{u}_2\} = - \begin{pmatrix} u_1 \partial_r u_2 + (v_1/r)(\partial_\theta u_2 - v_2) + w_1 \partial_z u_2 \\ u_1 \partial_r v_2 + (v_1/r)(\partial_\theta v_2 + u_2) + w_1 \partial_z v_2 \\ u_1 \partial_r w_2 + (v_1/r) \partial_\theta w_2 + w_1 \partial_z w_2 \end{pmatrix}. \tag{A25}$$

In the following, the notation  $\{\mathbf{u}_1, \mathbf{u}_2, m, k\}$  will designate the same column, except that the  $\partial_\theta$  and  $\partial_z$  terms are replaced by  $im$  and  $ik$ . With (9), Eq. (A23) becomes

$$\begin{aligned} \partial_t \mathbf{u}_{02} + \mathcal{M} \mathbf{u}_{02} + \nabla p_{02} &= A^2 e^{-2i\theta} e^{2ikz} \{\mathbf{u}_A, \mathbf{u}_A, -1, k\} + B^2 e^{+2i\theta} e^{2ikz} \{\mathbf{u}_B, \mathbf{u}_B, +1, k\} \\ &\quad + A \bar{B} e^{2ikz} \{\mathbf{u}_A, \mathbf{u}_B, +1, k\} + A \bar{A} (\{\mathbf{u}_A, \mathbf{u}_A, +1, -k\} + \{\mathbf{u}_A, \mathbf{u}_A, +1, -k\})/2 \\ &\quad + B \bar{B} (\{\mathbf{u}_B, \mathbf{u}_B, -1, -k\} + \{\mathbf{u}_B, \mathbf{u}_B, -1, -k\})/2 + A \bar{B} e^{-2i\theta} (\{\mathbf{u}_A, \mathbf{u}_B, -1, -k\} + \{\mathbf{u}_B, \mathbf{u}_A, -1, k\}) + \text{c.c.} \end{aligned} \tag{A26}$$

For  $\mathbf{u}_{02}$ , we look for a separable solution of the form

$$\begin{aligned} \mathbf{u}_{02}(r, \theta, z, t) &= A^2 e^{-2i\theta} e^{2ikz} \mathbf{r}_{AA}(r) + B^2 e^{+2i\theta} e^{2ikz} \mathbf{r}_{BB}(r) \\ &\quad + A \bar{B} e^{2ikz} \mathbf{r}_{AB}(r) + A \bar{A} \mathbf{r}_{A\bar{A}}(r) + B \bar{B} \mathbf{r}_{B\bar{B}}(r) \\ &\quad + A \bar{B} e^{-2i\theta} \mathbf{r}_{A\bar{B}}(r) + \text{c.c.} \end{aligned} \tag{A27}$$

The only terms that can be resonating in the forcing term are those related to  $A \bar{A}$ ,  $B \bar{B}$ , and their complex conjugates. As shown in Appendix B, the compatibility condition associated with these terms requires that they be zero in  $\mathbf{e}_\theta$  and  $\mathbf{e}_z$ . Yet it can be verified that, if  $\mathbf{u}_1$  and  $\mathbf{u}_2$  are two vectors of structure  $(iu, v, w)$  then  $\{\mathbf{u}_1, \mathbf{u}_2, m, k\}$  will be of structure  $(u, iv, iw)$ . The forcing terms related to  $A \bar{A}$  and  $B \bar{B}$  are, therefore, forced only in the  $\mathbf{e}_r$  direction. No compatibility condition needs to be imposed and we can set  $\mathbf{r}_{AA} = \mathbf{r}_{B\bar{B}} = 0$ . The amplitude equation is not modified at this order. This result is analogous to the one given by Greenspan<sup>25</sup> which concerns the case of a confined flow in solid body rotation.

All the vectors  $\mathbf{r}_{AA}$ ,  $\mathbf{r}_{BB}$ ,  $\mathbf{r}_{AB}$ , and  $\mathbf{r}_{A\bar{B}}$  are of the  $(iu, v, w)$  type and a careful check shows that the following symmetries hold:

$$\mathbf{r}_{AA} = (iu_{r_{AA}}, v_{r_{AA}}, w_{r_{AA}}), \quad \mathbf{r}_{BB} = (-iu_{r_{AA}}, v_{r_{AA}}, -w_{r_{AA}}), \tag{A28}$$

$$\mathbf{r}_{A\bar{B}} = (iu_{r_{A\bar{B}}}, v_{r_{A\bar{B}}}, 0), \quad \mathbf{r}_{AB} = (0, v_{r_{AB}}, 0). \tag{A29}$$

These functions are obtained from the following equations:

$$\mathcal{M}_{-2} \mathbf{r}_{AA} + \nabla_{-2,2k} p_{r_{AA}} = \{\mathbf{u}_A, \mathbf{u}_A, -1, k\}, \tag{A30}$$

$$\text{div}_{-2,2k} \mathbf{r}_{AA} = 0, \tag{A31}$$

$$\mathcal{M}_0 \mathbf{r}_{AB} + \nabla_{0,2k} p_{r_{AB}} = \{\mathbf{u}_A, \mathbf{u}_B, 1, k\} + \{\mathbf{u}_B, \mathbf{u}_A, -1, k\}, \tag{A32}$$

$$\text{div}_{0,2k} \mathbf{r}_{AB} = 0, \tag{A33}$$

$$\begin{aligned} \mathcal{M}_{-2} \mathbf{r}_{A\bar{B}} + \nabla_{-2,0} p_{r_{A\bar{B}}} &= \{\mathbf{u}_A, \mathbf{u}_B, -1, -k\} \\ &\quad + \{\mathbf{u}_B, \mathbf{u}_A, -1, k\}, \end{aligned} \tag{A34}$$

$$\text{div}_{-2,0} \mathbf{r}_{A\bar{B}} = 0. \tag{A35}$$

All the linear operators on the left-hand-side of these equations are not degenerate, so that the solutions exist and are unique. These functions are displayed in Figs. 9–11 in the case  $k = 2.261$ .

**3. Order  $\epsilon^0 \alpha^3$**

At order  $\epsilon^0 \alpha^3$ , we obtain the following inhomogeneous equation:

$$\partial_t \mathbf{u}_{03} + \mathcal{M} \mathbf{u}_{03} + \nabla p_{03} = \{\mathbf{u}_{01}, \mathbf{u}_{02}\} + \{\mathbf{u}_{02}, \mathbf{u}_{01}\}, \tag{A36}$$

$$\text{div } \mathbf{u}_{03} = 0. \tag{A37}$$

With (9) and (A27), the resonating forcing terms are

$$\begin{aligned} \partial_t \mathbf{u}_{03} + \mathcal{M} \mathbf{u}_{03} + \nabla p_{03} = & A|A|^2 e^{-i\theta} e^{ikz} (\{\overline{\mathbf{u}}_A, \mathbf{r}_{AA}, -2, 2k\} + \{\mathbf{r}_{AA}, \overline{\mathbf{u}}_A, +1, -k\}) + B|B|^2 e^{+i\theta} e^{ikz} (\{\overline{\mathbf{u}}_B, \mathbf{r}_{BB}, +2, 2k\} \\ & + \{\mathbf{r}_{BB}, \overline{\mathbf{u}}_B, -1, -k\}) + A|B|^2 e^{-i\theta} e^{ikz} (\{\overline{\mathbf{u}}_B, \mathbf{r}_{AB}, 0, 2k\} + \{\mathbf{r}_{AB}, \overline{\mathbf{u}}_B, -1, -k\} \\ & + \{\overline{\mathbf{u}}_B, \mathbf{r}_{AB}, -2, 0\} + \{\mathbf{r}_{AB}, \overline{\mathbf{u}}_B, +1, k\}) + B|A|^2 e^{+i\theta} e^{ikz} (\{\overline{\mathbf{u}}_A, \mathbf{r}_{AB}, 2, 0\} \\ & + \{\mathbf{r}_{AB}, \overline{\mathbf{u}}_A, -1, k\} + \{\overline{\mathbf{u}}_A, \mathbf{r}_{AB}, 0, 2k\} + \{\mathbf{r}_{AB}, \overline{\mathbf{u}}_A, +1, -k\}) + \text{c.c.} + \dots \end{aligned} \tag{A38}$$

To ensure the compatibility conditions, we make  $A$  and  $B$  depend on a slow time based on  $1/\alpha^2$

$$\frac{dA}{dt} = -i\alpha^2 A (b|A|^2 + c|B|^2), \tag{A39}$$

$$\frac{dB}{dt} = +i\alpha^2 B (c|A|^2 + b|B|^2), \tag{A40}$$

where

$$-ib = \frac{\langle \mathbf{u}_A^\perp, \{\overline{\mathbf{u}}_A, \mathbf{r}_{AA}, -2, 2k\} + \{\mathbf{r}_{AA}, \overline{\mathbf{u}}_A, +1, -k\} \rangle}{\langle \mathbf{u}_A^\perp, \mathbf{u}_A \rangle}, \tag{A41}$$

$$-ic = \frac{\langle \mathbf{u}_A^\perp, \{\overline{\mathbf{u}}_B, \mathbf{r}_{AB}, -2, 0\} + \{\mathbf{r}_{AB}, \overline{\mathbf{u}}_B, +1, k\} + \{\overline{\mathbf{u}}_B, \mathbf{r}_{AB}, 0, 2k\} + \{\mathbf{r}_{AB}, \overline{\mathbf{u}}_B, -1, -k\} \rangle}{\langle \mathbf{u}_A^\perp, \mathbf{u}_A \rangle}. \tag{A42}$$

We can easily check that the constants  $b$  and  $c$  are real. The numerical values of these constants are given in Table I.

**4. Determination of the order of magnitude of  $\alpha$**

By grouping the amplitude equation (A13), (A17) obtained at order  $\alpha\epsilon$  with those (A39), (A40) obtained at order  $\alpha^3$ , we can determine the order of magnitude  $\alpha$  of the per-

turbation so that the two physical phenomena (instability on the characteristic time scale  $1/\epsilon$  and phase dynamics for the Kelvin waves on the time scale  $1/\alpha^2$ ) act on a common time scale:

$$\alpha^2 = \epsilon, \tag{A43}$$

and therefore

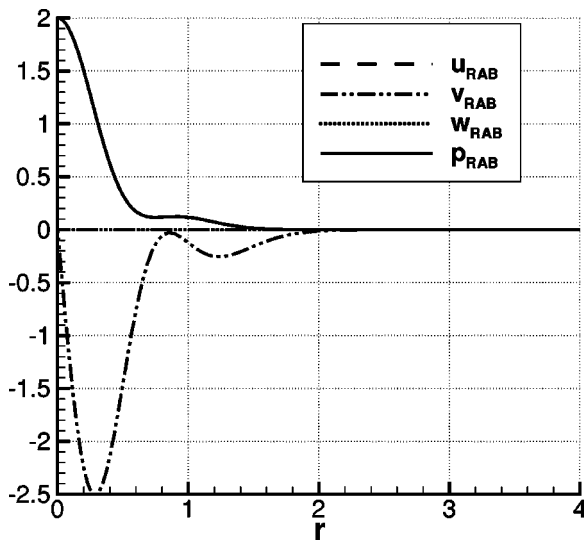


FIG. 10. Velocity and pressure fields of  $e^{2ikz} \mathbf{r}_{AB}(r)$ . Case  $k=2.261$ .

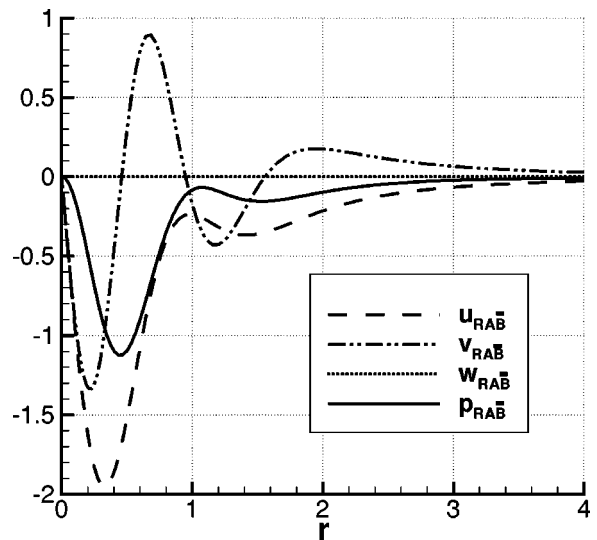


FIG. 11. Velocity and pressure fields of  $e^{-2i\theta} \mathbf{r}_{AB}(r)$ . Case  $k=2.261$ .

$$\frac{dA}{dt} = +i\epsilon aB - iA\epsilon(b|A|^2 + c|B|^2), \tag{A44}$$

$$\frac{dB}{dt} = -i\epsilon aA + iB\epsilon(c|A|^2 + b|B|^2). \tag{A45}$$

**5. Mean flow**

**a. Energy conservation**

We will now see that these amplitude equations do not conserve energy at order  $\epsilon$ . The energy of the flow contained in the domain  $0 \leq z \leq 2\pi/k$ , which corresponds to one wavelength, is based on the following scalar product:

$$[\mathbf{u}_1, \mathbf{u}_2] = \int_0^{2\pi/k} \int_0^{2\pi} \langle \mathbf{u}_1, \mathbf{u}_2 \rangle dz d\theta. \tag{A46}$$

We thus obtain the following terms for the energy:

$$E = [\mathbf{u}, \mathbf{u}] = \underbrace{[\mathbf{u}_0, \mathbf{u}_0]}_{O(1)} + 2\alpha \underbrace{[\mathbf{u}_0, \mathbf{u}_{01}]}_{O(\sqrt{\epsilon})} + \underbrace{\alpha^2 [\mathbf{u}_{01}, \mathbf{u}_{01}] + 2\epsilon [\mathbf{u}_0, \mathbf{u}_1] + 2\alpha^2 [\mathbf{u}_0, \mathbf{u}_{02}] + \dots}_{O(\epsilon)}. \tag{A47}$$

The energy is conserved at order  $O(1)$ , and at order  $O(\sqrt{\epsilon})$  since the interaction energy between the axisymmetrical vortex and the Kelvin waves  $A$  and  $B$  is zero,  $[\mathbf{u}_0, \mathbf{u}_{01}] = 0$ , but is not at order  $\epsilon$ . As a matter of fact, the energy at order  $\epsilon$  is  $E_\epsilon = \epsilon(K|A|^2 + K|B|^2)$  in which  $K = 8\pi^2/k \langle \mathbf{u}_A, \mathbf{u}_A \rangle$ . Thus  $d/dt E_\epsilon = -\epsilon^2 i(A\bar{B} - \bar{A}B)(2aK)$ . This term is not zero, and so the energy of this system is not conserved at this order. Physically speaking, this is due to the fact that the instability draws its energy from the axisymmetrical mean field. We will now see that we have to add an axisymmetrical mean field term at order  $\alpha^2 = \epsilon$  in the expansion (1) to allow the total energy to be conserved at order  $\epsilon$ . The time-evolution equation of this field will be determined at order  $\epsilon\alpha^2$  by a compatibility condition.

**b. Order  $\epsilon^1 \alpha^2$**

At order  $\epsilon^1 \alpha^2$ , we get the following equation:

$$\partial_t \mathbf{u}_{12} + \mathcal{M} \mathbf{u}_{12} + \nabla p_{12} = -\partial_{\tau'} \mathbf{u}_{02} + e^{+2i\theta} \mathcal{N} \mathbf{u}_{02} + e^{-2i\theta} \bar{\mathcal{N}} \bar{\mathbf{u}}_{02} + \{\mathbf{u}_{01}, \mathbf{u}_{11}\} + \{\mathbf{u}_{11}, \mathbf{u}_{01}\}, \tag{A48}$$

$$\text{div } \mathbf{u}_{12} = 0, \tag{A49}$$

where  $\tau'$  is the slow time  $t = (1/\epsilon)\tau'$ . According to (9), (A5), and (A27), only the following term in  $A\bar{B}$  and its conjugate are likely to resonate here:

$$\begin{aligned} \partial_t \mathbf{u}_{12} + \mathcal{M} \mathbf{u}_{12} + \nabla p_{12} &= A\bar{B} [\mathcal{N}_{-2} \mathbf{r}_{A\bar{B}} + \{\mathbf{u}_A, \bar{\mathbf{s}}_{-1}, +1, -k\} \\ &+ \{\bar{\mathbf{s}}_{-1}, \mathbf{u}_A, -1, k\} + \{\bar{\mathbf{u}}_B, \mathbf{s}_{+1}, +1, k\} \\ &+ \{\mathbf{s}_{+1}, \bar{\mathbf{u}}_B, -1, -k\}] + \text{c.c.} + \dots \end{aligned} \tag{A50}$$

The compatibility condition entails that the sum of the term in  $A\bar{B}$  and  $\bar{A}B$  must be zero in the  $\mathbf{e}_\theta$  and  $\mathbf{e}_z$  directions. A careful check shows that this sum has the following structure:

$$A\bar{B} \begin{pmatrix} f_r \\ if_\theta \\ 0 \end{pmatrix} + \bar{A}B \begin{pmatrix} f_r \\ -if_\theta \\ 0 \end{pmatrix} = \begin{pmatrix} (A\bar{B} + \bar{A}B)f_r \\ i(A\bar{B} - \bar{A}B)f_\theta \\ 0 \end{pmatrix}, \tag{A51}$$

so that a nonzero term exists in the  $\mathbf{e}_\theta$  direction. We therefore introduce in expansion (1) the following additional axisymmetrical term at order  $\alpha^2 = \epsilon$ :  $\alpha^2 \mathbf{u}_C = \alpha^2 C \mathbf{t}(r)$ .  $C$  is an amplitude varying slowly on a time scale  $1/\epsilon$  and  $\mathbf{t}(r)$  is the vector

$$\mathbf{t}(r) = (0, \Sigma(r), 0). \tag{A52}$$

The terms  $C$  and  $\mathbf{t}(r)$  are real and are determined so as to make the  $\mathbf{e}_\theta$  component vanish in the forcing term

$$\frac{dC}{dt} = i\epsilon(A\bar{B} - \bar{A}B), \tag{A53}$$

$$\Sigma(r) = f_\theta. \tag{A54}$$

The evaluation of  $f_\theta$  yields

$$\begin{aligned} \Sigma(r) = &-\frac{1}{r^2} \partial_r [r^2 (-f/2r) v_{rA\bar{B}} + (1/4) u_{rAB} df/dr \\ &- 2u_{s_{-1}} v_A + 2u_A v_{s_{-1}}]. \end{aligned} \tag{A55}$$

The mean flow  $\Sigma(r)$  is given in Fig. 3 in the cases  $k = 2.261, 3.958, 5.612$ .

**c. Final amplitude equations**

The mean field of order of magnitude  $\alpha^2 = \epsilon$  introduced above will modify the amplitude equations at order  $\alpha^3$

$$\frac{dA}{dt} = +i\epsilon aB - iA\epsilon(b|A|^2 + c|B|^2 + dC), \tag{A56}$$

$$\frac{dB}{dt} = -i\epsilon aA + iB\epsilon(c|A|^2 + b|B|^2 + dC), \tag{A57}$$

$$\frac{dC}{dt} = i\epsilon(A\bar{B} - \bar{A}B), \tag{A58}$$

with:

$$-id = \frac{\langle \mathbf{u}_A^\dagger, \{\mathbf{u}_A, \mathbf{t}, 0, 0\} + \{\mathbf{t}, \mathbf{u}_A, -1, k\} \rangle}{\langle \mathbf{u}_A^\dagger, \mathbf{u}_A \rangle}, \tag{A59}$$

where  $\mathbf{t}(r)$  was given in (A52) and (A55). The numerical values of  $d$  are given in Table I in the cases  $k = 2.261, 3.958, 5.612$ . The amplitude equations (A56)–(A58) allow conservation of energy at order  $\epsilon$  because a new interaction term exists between the axisymmetrical vortex and the created mean field:  $2\alpha^2 [\mathbf{u}_0, \mathbf{u}_C] = (8\pi^2/k) \langle \mathbf{u}_0, \mathbf{t} \rangle \alpha^2 C$ . The energy at order  $\epsilon$  is, therefore:  $E_\epsilon = \epsilon(K|A|^2 + K|B|^2 + K_C C)$  in which  $K_C = (8\pi^2/k) \langle \mathbf{u}_0, \mathbf{t} \rangle$ . Its derivative as a function of time is:  $(d/dt)E_\epsilon = -\epsilon^2 i(A\bar{B} - \bar{A}B)(2aK - K_C)$ . This is zero when  $K_C = 2aK$ , i.e.,

$$\langle \mathbf{u}_0, \mathbf{t} \rangle = 2a \langle \mathbf{u}_A, \mathbf{u}_A \rangle. \tag{A60}$$

In Table I, we have given in the cases  $k=2.261, 3.958, 5.612$  the numerical values of  $\langle \mathbf{u}_0, \mathbf{t} \rangle$  and  $2a\langle \mathbf{u}_A, \mathbf{u}_A \rangle$ . We check that these quantities are equal with a precision of four digits. This allows us to check that the computation of  $\mathbf{t}$  is valid. The conservation of energy at order  $\epsilon$ , therefore, reads

$$|A|^2 + |B|^2 + 2aC = \text{cst.} \quad (\text{A61})$$

## APPENDIX B: SOME RESULTS ON THE LINEAR INHOMOGENEOUS EQUATION

In this Appendix, we present some results concerning the inhomogeneous linear equation mentioned in the course of the weakly nonlinear analysis. For any integer  $m$  and any real  $k$ , we consider the following problem:

$$\mathcal{M}_m \mathbf{u} + \nabla_{m,k} p = \mathbf{f}(r), \quad (\text{B1})$$

$$\text{div}_{m,k} \mathbf{u} = 0, \quad (\text{B2})$$

where  $\mathcal{M}_m$ ,  $\nabla_{m,k}$ , and  $\text{div}_{m,k}$  are defined in Sec. III.  $\mathbf{f}(r)$  is a forcing term whose structure is the following:

$$\mathbf{f}(r) = (f_r, if_\theta, if_z), \quad (\text{B3})$$

where  $f_r$ ,  $f_\theta$ , and  $f_z$  are real functions. The following boundary conditions are joined to the problem:  $\mathbf{u}(r) \rightarrow 0$  when  $r \rightarrow +\infty$  and  $\mathbf{u}(r)$  bounded when  $r \rightarrow 0$ . We look for a solution of the form

$$\mathbf{u} = (iu, v, w). \quad (\text{B4})$$

The homogeneous equation determines the stationary Kelvin waves of the axisymmetrical vortex. Depending on the parameters  $(m, k)$ , the homogeneous equation can thus be degenerate and compatibility conditions for the forcing term  $\mathbf{f}(r)$  must be satisfied in order for the inhomogeneous equation to have a solution.

In the next section, we examine the particular case  $m=0$  and  $k=0$ . We show that two compatibility conditions for the forcing term  $\mathbf{f}$  arise. In the general case, we then show that the inhomogeneous linear equations (B1) and (B2) may be reduced to a system governing only the radial component of  $\mathbf{u}$  and the pressure  $p$ . In the last section, we discretize this system thanks to a Chebyshev–Gauss collocation method. The solutions to Eqs. (B1) and (B2) are obtained thanks to Lower-Upper (LU) type decompositions. Note that the same methods are used to obtain the adjoint eigenmodes.

### 1. Particular case: $m=0$ and $k=0$

The equations determining the solution (B4) of Eqs. (B1) and (B2) are

$$-2\Omega v + \partial_r p = f_r, \quad (\text{B5})$$

$$(2\Omega + rd\Omega/dr)u = f_\theta, \quad (\text{B6})$$

$$0 = f_z, \quad (\text{B7})$$

$$\partial_r(ru) = 0. \quad (\text{B8})$$

Hence,  $u=0$ , so that  $f_\theta=0$ . Two compatibility conditions exist in this case

$$f_\theta = f_z = 0. \quad (\text{B9})$$

## 2. General case

Equations (B1) and (B2) reduce to

$$\frac{d}{dr} \begin{pmatrix} u \\ p \end{pmatrix} = \begin{pmatrix} -\frac{1}{r} + \frac{2\Omega + rd\Omega/dr}{r\Omega} & \frac{k^2 + m^2/r^2}{m\Omega} \\ m\Omega - \frac{2(2\Omega + rd\Omega/dr)}{m} & -\frac{2}{r} \end{pmatrix} \begin{pmatrix} u \\ p \end{pmatrix} + \begin{pmatrix} -\frac{kf_z}{m\Omega} - \frac{f_\theta}{r\Omega} \\ f_r + \frac{2f_\theta}{m} \end{pmatrix}, \quad (\text{B10})$$

$$v = \frac{f_\theta - (2\Omega + rd\Omega/dr)u - mp/r}{m\Omega}, \quad (\text{B11})$$

$$w = \frac{f_z - kp}{m\Omega}. \quad (\text{B12})$$

## 3. Spatial discretization

The space-derivatives are discretized by a spectral collocation method with Chebyshev polynomials. The differential equations in (B10) are given on the interval  $0 < r < +\infty$ . We map this interval on  $-1 < \hat{r} < +1$  with the function<sup>26</sup>

$$r = -H \log \frac{1 - \hat{r}}{2}. \quad (\text{B13})$$

We choose the Gauss collocation points

$$\hat{r}_i = \cos \frac{(2i+1)}{2N+2} \pi, \quad i=0 \dots N. \quad (\text{B14})$$

These points do not include the edges  $\hat{r} = \pm 1$ , so that no boundary conditions will be specified in the following. The chosen function basis, i.e., the  $N+1$  Chebyshev polynomials, and Eq. (B10) naturally select the right solutions, i.e., solutions  $\mathbf{u}$  such that  $\mathbf{u} \rightarrow 0$  when  $r \rightarrow \infty$  and  $\mathbf{u}$  bounded when  $r \rightarrow 0$ .

Numerically, if we let  $N=30, H=1$ , we already get excellent results. We then used  $N=100, H=2$  to confirm the results.

## 4. LU decomposition

The various problems are solved by constructing a matrix from the discretization of Eq. (B10) and breaking it down in the LU form.

Solutions to the homogeneous equation are sought by considering the last row from the Gauss pivot. A Newton-type descent method is used to adjust  $k$  such that the last coefficient from the pivot is zero. This is achieved only for specific values of  $k$ . This method is applied here for determining the stationary Kelvin waves.

The inhomogeneous linear equation is also solved by using the LU decomposition. When the linear operator is degenerate, the projection of the forcing term on the kernel of the linear operator has to be zero. The last row from the

Gauss pivot therefore has to be zero for the forcing term in order for the compatibility condition to hold. We use this as a numerical check in our computations.

- <sup>1</sup>T. Leweke and C. H. K. Williamson, "Cooperative elliptic instability of a vortex pair," *J. Fluid Mech.* **360**, 85 (1998).
- <sup>2</sup>S. C. Crow, "Stability theory of a pair of trailing vortices," *AIAA J.* **8**, 2172 (1970).
- <sup>3</sup>D. W. Moore and P. G. Saffman, "Structure of a line vortex in an imposed strain," in *Aircraft Wake Turbulence and its Detection*, edited by J. H. Olsen, A. Goldberg, and M. Rogers (Plenum, New York-London, 1971), pp. 339–354.
- <sup>4</sup>S. E. Widnall and D. B. Bliss, "Slender-body analysis of the motion and stability of a vortex filament containing an axial flow," *J. Fluid Mech.* **50**, 335 (1971).
- <sup>5</sup>S. E. Widnall, D. Bliss, and A. Zalay, "Theoretical and experimental study of the stability of a vortex pair," in *Aircraft Wake Turbulence and its Detection*, edited by J. H. Olsen, A. Goldberg, and M. Rogers (Plenum, New York-London, 1971), pp. 305–338.
- <sup>6</sup>D. W. Moore and P. G. Saffman, "The motion of a vortex filament with axial flow," *Philos. Trans. R. Soc. London, Ser. A* **272**, 403 (1972).
- <sup>7</sup>D. W. Moore and P. G. Saffman, "Axial flow in laminar trailing vortices," *Proc. R. Soc. London, Ser. A* **333**, 491 (1973).
- <sup>8</sup>D. W. Moore and P. G. Saffman, "The instability of a straight vortex filament in a strain field," *Proc. R. Soc. London, Ser. A* **346**, 413 (1975).
- <sup>9</sup>C.-Y. Tsai and S. E. Widnall, "The stability of short waves on a straight vortex filament in a weak externally imposed strain field," *J. Fluid Mech.* **73**, 721 (1976).
- <sup>10</sup>C. Eloy and S. Le Dizès, "Three-dimensional instability of Burgers and Lamb–Oseen vortices in a strain field," *J. Fluid Mech.* **378**, 145 (1999).
- <sup>11</sup>R. T. Pierrehumbert, "Universal short-wave instability of two-dimensional eddies in an inviscid fluid," *Phys. Rev. Lett.* **57**, 2157 (1986).
- <sup>12</sup>B. J. Bayly, "Three-dimensional instability of elliptical flow," *Phys. Rev. Lett.* **57**, 2160 (1986).
- <sup>13</sup>F. Waleffe, "On the three-dimensional instability of strained vortices," *Phys. Fluids A* **2**, 76 (1990).
- <sup>14</sup>D. Meiron, M. Shelley, W. Ashurst, and S. Orszag, "Numerical studies on vortex reconnection," in *Mathematical Aspects of Vortex Dynamics*, edited by R. Caflisch (SIAM, Philadelphia, 1989), pp. 183–194.
- <sup>15</sup>R. Klein and A. J. Majda, "An asymptotic theory for the nonlinear instability of antiparallel pairs," *Phys. Fluids A* **5**, 369 (1993).
- <sup>16</sup>R. Klein, A. J. Majda, and K. Damodaran, "Simplified equations for the interaction of nearly parallel vortex filaments," *J. Fluid Mech.* **288**, 201 (1995).
- <sup>17</sup>P. Orlandi, G. F. Carnevale, S. K. Lele, and K. Shariff, "DNS study of stability of trailing vortices," *Proceedings of the Summer Program 1998* (Center for Turbulence Research, Stanford, 1998).
- <sup>18</sup>W. V. R. Malkus, "An experimental study of the global instabilities due to the tidal (elliptical) distortion of a rotating elastic cylinder," *Geophys. Astrophys. Fluid Dyn.* **48**, 123 (1989).
- <sup>19</sup>F. Waleffe, *The 3D instability of a strained vortex and its relation to turbulence*, Ph.D. thesis, Massachusetts Institute of Technology, 1989.
- <sup>20</sup>R. R. Kerswell, "Secondary instabilities in rapidly rotating flows: inertial wave breakdown," *J. Fluid Mech.* **382**, 283 (1999).
- <sup>21</sup>D. M. Mason and R. R. Kerswell, "Non-linear evolution of the elliptical instability," *J. Fluid Mech.* **396**, 73 (1999).
- <sup>22</sup>J. Guckenheimer and A. Mahalov, "Instability induced by symmetry reduction," *Phys. Rev. Lett.* **68**, 2257 (1992).
- <sup>23</sup>E. Knobloch, A. Mahalov, and J. Marsden, "Normal forms for three-dimensional parametric instabilities in ideal hydrodynamics," *Physica D* **73**, 49 (1994).
- <sup>24</sup>N. Lebovitz and K. Saldanha, "On the weakly nonlinear development of the elliptic instability," *Phys. Fluids* **11**, 3374 (1999).
- <sup>25</sup>H. P. Greenspan, "On the non-linear interaction of inertial modes," *J. Fluid Mech.* **36**, 257 (1969).
- <sup>26</sup>C. Canuto, M. Y. Hussaini, A. Quateroni, and T. A. Zang, *Spectral Methods in Fluid Dynamics* (Springer-Verlag, Berlin Heidelberg, 1988).